

# Beam Alignment and Tracking for Autonomous Vehicular Communication using IEEE 802.11ad-based Radar

<sup>1</sup>Guillem Reus Muns, <sup>2</sup>Kumar Vijay Mishra, <sup>3</sup>Carlos Bocanegra Guerra, <sup>4</sup>Yonina C. Eldar and <sup>5</sup>Kaushik R. Chowdhury  
<sup>1,3,5</sup>Electrical and Computer Engineering Department, Northeastern University, Boston, MA, USA  
<sup>2,4</sup>Andrew and Erna Viterbi Faculty of Electrical Engineering, Technion - Israel Institute of Technology, Haifa, Israel  
 Email: {<sup>1</sup>greusmuns@coe, <sup>3</sup>bocanegrac@coe, <sup>5</sup>krc@ece}.neu.edu, {<sup>2</sup>mishra, <sup>4</sup>yonina}@ee.technion.ac.il

**Abstract**—Mobility scenarios involving short contact times pose a challenge for high bandwidth data transfer between autonomous vehicles and roadside base stations (BS). Millimeter wave bands are a viable solution as they offer enormous bandwidth in the 60GHz band with several Gbps data transfer rates. However, beamforming is used as a default mode in this band, which requires accurate and continuous alignment under relative motion. We propose a method in which an off-the-shelf IEEE 802.11ad WiFi router is configured to serve as the BS as well as a radar exploiting special structure of 802.11ad preamble. We embed the radar functionality within standards-compliant operations that do not modify the core structure of the frames beyond what is defined by the 802.11ad protocol. This not only reduces the beam training time, but also ensures scalability with increasing vehicular traffic because radar allows accurate ranging of up to 0.1m at distances up to 200m. We further analyze the ensuing cost-benefit trade-off between the time allotted to the proposed in-band radar and communication modes. Our results reveal 83% reduction on the overhead incurred during the beam training achieved for a specific simulated vehicular scenario over the classical 802.11ad operation.

**Index Terms**—IEEE 802.11ad, mmWave, automotive radar, beam alignment, CAV

## I. INTRODUCTION

Connected and autonomous vehicles are being gradually integrated into consumer-level road transportation given the associated cost/energy savings, as well as increase safety and comfort. In addition, several companies use the same technology to generate digital maps and real-time 3-D visuals through real-time sensing, which can improve offline path planning algorithms. Each of these examples requires efficient relaying of large volumes of data by the vehicles, ranging in the order of several gigabits-per-second. The key problem that we address in this paper is how to devise a cost-effective communication architecture for vehicle-to-infrastructure (V2I) that offers high data capacity while being resilient to the challenges posed by mobility.

Millimeter Wave (mmWave) technology in the recently opened 57 – 64 GHz band is a promising candidate for our scenario because of the availability of massive unlicensed spectrum. Consumer-exploitation of this band is already underway: The IEEE 802.11ad standard enables throughput of up to 7 Gbps at 60 GHz for short-range wireless communication [1]. Although the available bandwidth is considerably wider in these bands (for e.g., IEEE 802.11ad defines up to 2 GHz wide channels), transmissions suffer from

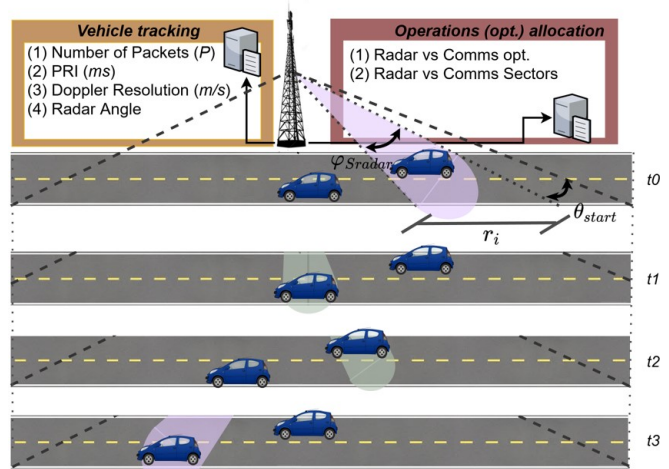


Fig. 1. V2I scenario where a BS uses radar to localize and serve vehicles moving right to left. Radar operations (purple) allow for determining the location and speed, enabling directive and robust data transfer (green). These operations are scheduled within a standard MAC frame given in Fig. 2.

high attenuation associated with increasing carrier frequency and channel losses arising from natural phenomena such as atmospheric absorption. In order to overcome these problems, highly directional antennas are used. Here, the radiation beam patterns are configured to ensure the peak of the transmitted RF energy appears along the intended direction, while lowering the emissions in other locations.

However, narrow beams efficiently focus energy in the chosen direction, but are less robust to movement. Also, blockage plays a major role compared with sub-6 GHz bands. Finally, the beam training procedure is time-consuming and lowers efficiency by utilizing network resources that could be used for communication. This worsens in mobile scenarios where the beam training function calls are frequent [2].

• **Proposed Approach:** Our approach performs both radar operations and conventional communication using a common transmitter/receiver (Tx/Rx) chain (Fig. 1) with 802.11ad physical layer (PHY) frames, as proved earlier in [3, 4]. Additionally, we extend further to the Media Access Control (MAC) layer by integrating these functions within defined MAC protocol headers (see Fig. 2), without any protocol

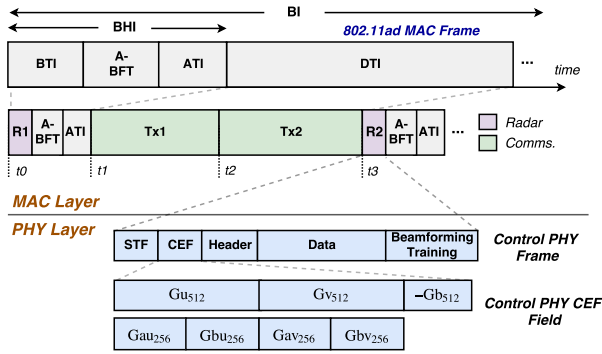


Fig. 2. The 802.11ad MAC frame configured to accommodate radar operations. R1 and R2 represent the radar periods while Tx1 and Tx2 are for the vehicle data transfer.

modification.

Our main contributions are:

- 1) We design and profile a 802.11ad PHY-based radar in terms of Doppler resolution, which determines the accuracy of the radar, its ability to track the vehicles, and the required time of operation.
- 2) We connect an in-band radar ranging method with the classical 802.11ad operation, and study the associated cost-benefit trade-offs among the efficiency of channel utilization, throughput, beam dimensions, among others.
- 3) We propose a 802.11ad MAC configuration to accommodate radar operations alongside regular communications operations, without any change in the channel access operation. Consequently, this reduces misalignment in a high-mobility environment while maintaining low overhead.
- 4) We provide spatial characterization of the beamwidth, angular sector and sector overlap as a function of the radar performance, and analyze the resulting throughput when in-band radar and communication operations are performed using the same hardware.

This paper is organized as follows. Section II reviews the state of the art. Section III describes the technical details of the proposed 802.11ad-based radar, which influences the parameters used in the later sections. Section IV contains a detailed analysis of the achievable throughput. In Section V, we provide an operational description of the vehicular scenario and connect the technical development to the application scenario. Section VI gives the performance evaluation and, finally, Section VII concludes the paper.

## II. RELATED WORK

Many recent research efforts have been devoted to reducing the beam training overhead in the mmWave band. In [5], the authors reduce the time for beam training using in-packet BF. In [6], a codebook design scheme enhances the system performance. While the above mentioned works reduce the overhead of beam training, they are not designed for mobility situations. Recent work involving mobility leverages out-of-band position reports to aid in beam training [2, 7]. We use the same (IEEE 802.11ad) band to obtain such reports.

The IEEE 802.11ad physical layer transmits control (CPHY), single carrier (SC) and orthogonal frequency-division multiplexing (OFDM) modulation frames at chip rates of 1.76 GHz and 2.64 GHz, respectively. Each IEEE 802.11ad CPHY and SCPHY frame consist of a short training field (STF), a channel estimation field (CEF), header, data and a beamforming training field (see Fig. 2). The CPHY and SCPHY frames have the same chip rate, carrier frequency and CEF structure. However, the CPHY STF is longer than that of the SCPHY. The STF and CEF together form the corresponding (CPHY or SCPHY) preambles. Within the CEF lie two 512-point sequences  $G_{u512}[n]$  and  $G_{v512}[n]$  which encapsulate Golay pairs. These paired sequences have the property of perfect *aperiodic* autocorrelation (zero sidelobes) making them useful for communication channel estimation [3] and radar remote sensing [4]. In this paper, our radar employs 802.11ad CPHY/SCPHY frames to estimate the range and Doppler velocity of the vehicles.

Among prior studies, the closest to our work is [8] which employs radar for the beam-alignment but it does not specify any particular protocol for communication. In addition, it excludes high-mobility vehicles and the radar does not co-exist within the same band. In [4], an in-band radar that uses 802.11ad signaling is presented for vehicle-to-vehicle (V2V) applications. The model assumes a single target and estimates its range using SCPHY STF and symbol boundary detection (SBD), while a coarse estimation of Doppler velocity is obtained using the pulse-pair method [9, 10]. Very accurate estimates of radar range and Doppler velocity are obtained in [11] using a 5.89 GHz dedicated short-range communication (DSRC)-based V2V communication link. In [12], a general-purpose spectrum sharing radar is presented using the recently proposed concept of cognitive radar that exploits sub-Nyquist processing. The automotive radar application modifications are suggested in [13] but these works employ IEEE 802.22 cognitive radio for communications. In contrast to these works, we use 802.11ad-based pulse-Doppler radar for beam alignment and radar network synchronization without any restriction on mobility. Unlike [4, 14], our methods are applicable for both CPHY and SCPHY frames.

## III. 802.11AD V2I AUTOMOTIVE RADAR

A *Golay complementary pair* consists of two sequences  $G_{a_N}$  and  $G_{b_N}$  both of the same length  $N$  with entries  $\pm 1$ . Consequently, their *aperiodic* autocorrelation functions have sidelobes equal in magnitude but opposite in sign. Therefore, the sum of the two autocorrelations has a peak of  $2N$  and a sidelobe level of zero:

$$G_{a_N}[n] * G_{a_N}[-n] + G_{b_N}[n] * G_{b_N}[-n] = 2N\delta[n], \quad (1)$$

where  $*$  denotes linear convolution. The 802.11ad CEF transmit signal is a concatenated sequence:

$$s_T[n] = G_{u512}[n] + G_{v512}[n - 512], \quad n = 0, 1, \dots, 1023. \quad (2)$$

Each of the sequences  $G_{u512}[n]$  and  $G_{v512}[n]$  contains a Golay complementary pair of length 256,  $\{G_{au256}, G_{bu256}\}$  and  $\{G_{av256}, G_{bv256}\}$ , respectively. The discrete-time sequence  $s_T[n]$  is passed through a digital-to-analog-converter (DAC)

the output of which can be represented as a weighted sum of Dirac impulses  $s_T(t) = \sum_m s_T[m]\delta(t - mT_c)$ . The baseband signal is then upconverted for transmission:  $x(t) = s_T(t)e^{j2\pi f_c t}$ , where  $f_c$  denotes the carrier frequency.

Suppose the radar transmits  $P$  packets at the pulse repetition interval (PRI)  $T_p$  towards  $L$  direct-path nonfluctuating targets of complex reflectivity  $\alpha_l$  located at range  $d_l = c\tau_l/2$  and Doppler velocity  $v_l = 2\pi f_{D_l}$ , where  $c = 3 \times 10^8$  m/s is the speed of light,  $\tau_l$  is the time delay, and  $f_{D_l}$  is the associated Doppler frequency. Ignoring the multi-path components (MPC), the reflected received signal at the baseband, i.e., after down-conversion, is given by

$$\begin{aligned} x_R(t) &= \sum_{p=0}^{P-1} \sum_{l=1}^L \alpha_l x_T(t - \tau_l - pT_p) e^{-j2\pi f_{D_l} t} + z(t) \\ &\approx \sum_{p=0}^{P-1} \sum_{l=1}^L \alpha_l x_T(t - \tau_l - pT_p) e^{-j2\pi f_{D_l} pT_p} + z(t), \end{aligned} \quad (3)$$

where  $z(t)$  is additive circular-symmetric white Gaussian noise. The last approximation follows from the fact that  $f_{D_l} \ll 1/T_p$  so that the phase rotation within one coherent processing interval (CPI) ("slow time") can be approximated as a constant. Here, we have assumed that the coefficient  $\alpha_l$  also characterizes antenna directivity, processing gains and attenuations including path loss. The received signal is downconverted and sampled at  $F_c = 1/T_c$  to obtain

$$x_R[n] = x_R(nT_c) = \sum_{p=0}^{P-1} \sum_{l=1}^L \alpha_l s_T(nT_c - \tau_l - pT_p) e^{-j2\pi f_{D_l} pT_p} + z(nT_c) \quad (4)$$

The sampled signal is passed through matched filters of each Golay sequence e.g. for the first pair, we have

$$\begin{aligned} \hat{h}_{1au}[n] &= x_R[n] * Gau_{256}[-n] \\ \hat{h}_{1bu}[n] &= x_R[n] * Gbu_{256}[-n]. \end{aligned} \quad (5)$$

These outputs are delayed:  $\hat{h}_{1a}[n] = \hat{h}_{1au}[n]$ ,  $\hat{h}_{1b}[n] = \hat{h}_{1bu}[n + 256]$ , and summed up to yield the channel estimate

$$\begin{aligned} \hat{h}_1[n] &= \frac{1}{512} (\hat{h}_{1a}[n] + \hat{h}_{1b}[n]) \\ &\approx \frac{1}{512} \sum_{p=0}^{P-1} \sum_{l=1}^L \alpha_l \delta(nT_c - \tau_l - pT_p) e^{-j2\pi f_{D_l} pT_p} \\ &\quad + z[n] * (Gau_{256}[-n] + Gbu_{256}[-n]), \end{aligned} \quad (6)$$

where we assumed that the Doppler shifts are nearly identical for the two Golay sequences  $Gau_{256}$  and  $Gbu_{256}$  enabling us to use the Golay pair property (1). Another estimate  $\hat{h}_2[n]$  of the radar channel is available via the second Golay pair within  $Gv_{512}$ . An average of the two estimates yields a final approximation of the radar channel.

We discretize the range-time space in, say,  $N_R$  bins of resolution  $cT_c/2$ . We then create a delay-Doppler map by taking a  $P$ -point Discrete Fourier Transform (DFT) of the radar channel estimates corresponding to each delay bin. Then, the delay and radial (Doppler) frequencies of the targets are given by the location of the first  $L$  peaks on the delay-Doppler map.

At the carrier frequency  $f_c$  of 60 GHz, the wavelength is  $\lambda_c = c/f_c = 0.005$  m. The STF of CPHY and SCPHY frames

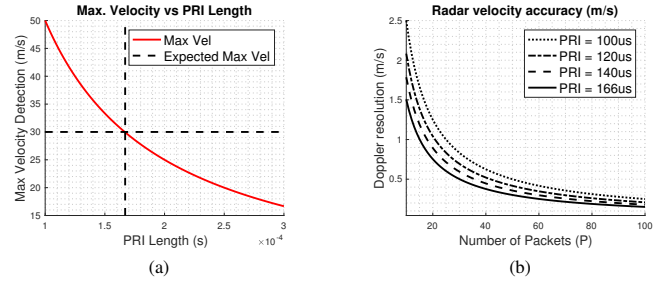


Fig. 3. (a) Maximum detectable velocity  $v_u$  as a function of the PRI length. For highways, where  $v_u = 30$  m/s, PRI shall be no greater than 0.166 ms. (b) The radar accuracy as a function of  $P$  for PRI no greater than the highway limit.

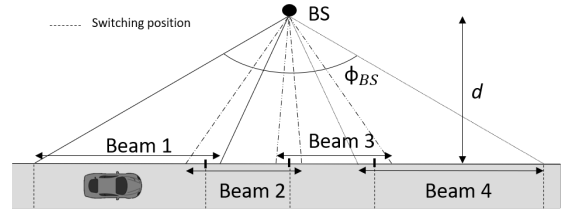


Fig. 4. Example of beam design with four beam.

contain 6400 and 2176 symbols, respectively. The CEF of both frames has 1152 symbols each. For the symbol time of  $T_c = 1/1.76e9 = 0.568$  ns, we obtain a minimum PRI of  $T_{pr} = T_c * (6400 + 1152) = 4.29 \mu s$  for CPHY while the same is  $1.89 \mu s$  for the SCPHY. A typical long range V2I radar (LRR) operates with a maximum unambiguous range of  $R_u = 200$  m and range resolution of 0.1 m. The symbol time of 802.11ad yields a good range resolution of  $\Delta R = cT_c/2 = 8.52$  cm.

If  $P$  packets are transmitted, then the CPI duration is  $T_{int} = PT_{pr}$ . For pulse repetition at a uniform rate, the maximum unambiguous Doppler velocity of the radar is given by  $v_u = \lambda_c/T_{pr}$  and the Doppler resolution obtained through Fourier processing is  $\Delta v = \lambda_c/(2T_{int})$ . Fig. 3 shows the dependence of the Doppler resolution on the number of packets and PRI. The total time the radar takes to scan a certain sector is:

$$t_{\text{radar}} \approx T_{\text{int}} \lfloor \varphi_{\text{Sradar}} / \theta_{\text{radar}} \rfloor, \quad (7)$$

where  $\lfloor \cdot \rfloor$  denotes the floor function,  $\theta_{\text{radar}}$  is the scan rate per unit CPI, fixed to  $0.5^\circ/\text{CPI}$ , and  $\varphi_{\text{Sradar}}$  is the sector size.

#### IV. 802.11AD PHY/MAC PROTOCOL CONFIGURATION

Consider a BS located at distance  $d$  from an ideal straight road, serving  $V$  number of non-stationary vehicles that pass along a fixed and uniform route (Fig. 4). Each vehicle  $c_l$  is characterized by its true location and velocity at time  $t$ ,  $y_l(t)$  and  $v_l(t)$ , respectively. The BS obtains the radar estimates  $\hat{d}_l(t)$  and  $\hat{v}_l(t)$  of the location and velocity, respectively. For simplicity,  $\hat{v}_l(t)$  will be assumed to be constant. As we describe below, the 802.11ad throughput is affected by the location of the vehicles with respect to the BS. Given the communication scenario (Fig. 1) and transmit power  $P_{\text{tx}}$ , we assume line-of-sight (LOS), allowing for a simplified expression for received power  $P_{\text{rx}}$  [2] (all quantities in dB):

$$P_{rx} = P_{tx} + G_{tx} - PL + G_{rx}, \quad (8)$$

where  $PL$  is the path loss and  $G_{tx}$  and  $G_{rx}$  are the antenna gains in transmission and reception, respectively. Further,

$$PL = 10n \log_{10} d_v + SF + C_{att} + A_{att} + R_{att}, \quad (9)$$

where  $n$  is the path loss exponent,  $d_v$  is the distance from the Tx in the BS to the vehicle, and  $SF$  corresponds to the random shadowing effect following a lognormal distribution  $SF \sim \mathcal{N}(0, \sigma^2)$  with  $\sigma = 5.8$ . The  $C_{att}$ ,  $A_{att}$  and  $R_{att}$  are the LOS link, atmospheric and rain attenuations, respectively. The linear scale antenna gains are given by

$$G_{tx/rx} = \frac{4 \cdot 180^2}{\theta_{el} \theta_{az} \pi}, \quad (10)$$

where  $\theta_{el}$  and  $\theta_{az}$  are the half-power beamwidths (radians) in elevation and azimuth for the corresponding antennas. To be consistent with the previous work in [2] and [7], we assumed ideal beamforming in (10), characterized by uniformly distributed gain within the beam and no side lobes.

We model the impairments at the receiver by accounting for the phase noise  $P_{noise}$  as

$$P_{noise} = N_{floor} + 10 \log_{10} B + NF, \quad (11)$$

where  $N_{floor}$  is the noise floor,  $B$  is the system bandwidth and  $NF$  the noise figure of the receiver chain. As a result, the SNR is a function of the Tx-Rx distance  $d_v$  and beamwidth:

$$SNR(\theta_{az}, d_v) = \frac{P_{rx}(\theta_{az}, d_v)}{P_{noise}}. \quad (12)$$

Here,  $\theta_{el}$  is fixed to a value that encompasses the width of the road. Hence, it depends on the distance  $d$ . Both  $\theta_{el}$  and  $\theta_{az}$  are assumed identical in transmission and reception.

For each Modulation and Coding Scheme (MCS), the 802.11ad standard requires a minimum Packet Error Rate (PER) which, in turn, is inherently impacted by the Signal-to-Noise Ratio (SNR). As in (12), the SNR itself depends on the scenario geometry  $d_v$  and  $\theta_{az}$ . We can express this dependency as a function  $SNR(\theta_{az}, d_v)$ . Further, the MCS-0 (most robust) demands a PER lower than a threshold ( $\gamma$ ) of 5% for a PHY service data unit (PSDU) length of 256 octets. For any other MCS, the PER shall be less than  $\gamma = 1\%$  for a PSDU length of 4096 octets [1]. Thus, the achievable throughput  $R_{802.11ad}$  is characterized by the tuple  $\{SNR, PER, MCS\}$ . To obtain the maximum data rate  $R$ , our approach always selects the MCS corresponding to the highest data rate among the ones that meet the PER requirements:

$$R(\theta_{az}, d_v) = \max_{\substack{MCS \\ PER(SNR(\theta_{az}, d_v)) \leq \gamma}} R_{802.11ad}(MCS). \quad (13)$$

The average data rate  $\bar{R}_l$ , or simply  $\bar{R}$ , between, say, a  $l$ th vehicle and the BS is computed as the integral of the achievable rate over the contact time interval  $[t_1, t_2]$ :

$$\bar{R} = \frac{1}{t_2 - t_1} \int_{t_1}^{t_2} R(t) dt. \quad (14)$$

For ease of notation, we rewrite  $[t_1, t_2]$  as  $[t_{init}, t_{init} + t_c]$ :

$$\bar{R} = \frac{1}{t_c} \int_{t_{init}}^{t_{init} + t_c} R(t) dt, \quad (15)$$

where  $t_{init}$  corresponds to the instant when the  $l$ th vehicle enters the area covered by the BS and  $t_c$  is the contact duration:

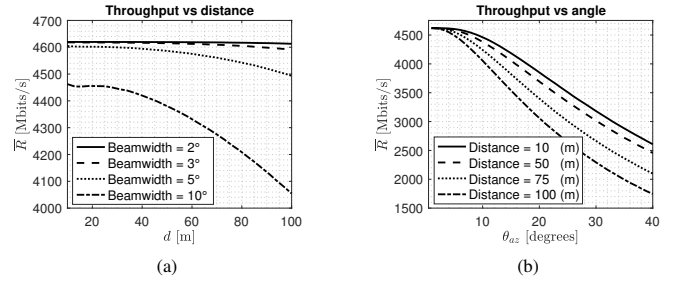


Fig. 5. Average throughput analysis with respect to the (a) BS-Road distance and (b) beamwidth.

$$t_c = \frac{2d \tan\left(\frac{\phi_{BS}}{2}\right)}{v_l}, \quad (16)$$

where  $\phi_{BS}$  is the BS coverage angle (see Fig. 4). From Fig. 5, we conclude following: First, a narrower beamwidth helps mitigate the high path loss attenuation, achieve a higher SNR and, in turn, increase the achievable throughput. Second, the achievable throughput is impacted more by the beamwidth  $\theta_{az}$  than the distance  $d$ . The latter finding serves as a design constraint in our system, i.e., *narrow beamwidth is preferred over short distances*.

## V. 802.11AD-BASED JOINT RADAR-COMMUNICATIONS

Consider the scenario in Fig. 4. The spatial orientation of the beams follow the beam-switching pattern [15]. Only one sector is activated at a time, and the BS either performs the radar or communication operations [7]. However, the respective sectors are defined differently: For communication, the adjacent sectors have some overlap that is specified by an overlap ratio parameter. The radar sectors do not overlap and their angular aperture is controlled by  $\varphi_{Sradar}$ . As stated in Section IV, the beams are assumed to be ideal, i.e., if at any instant a vehicle is not within the limits of the active sector, we consider the beams to be in complete misalignment.

The 802.11ad protocol structures its frames into Beacon Intervals (BI) (Fig. 2) with 30 ms duration for vehicular networks [2]. The BIs consist of Beacon Header Interval (BHI), where antenna beams are formed and network synchronization information is exchanged, and Data Transfer Interval (DTI), during which the actual communication occurs. On top of this, the protocol also defines a Beam Refinement Protocol (BRP) during the DTI, where a similar procedure is carried out with narrower beams. Three subintervals constitute BHI: *Beacon Transmission Interval (BTI)*, where Sector Level Sweep (SLS) is initialized, *Associated Beamforming Training (A-BFT)*, for the SLS finalization, and *Announcement Transmission Interval (ATI)*, where devices are allocated during the DTI.

We explain our PHY-MAC configuration through a scenario requiring vehicles to synchronize with a given BS that has radar capabilities. First, the BS sends  $P$  Directional Multi-Gigabit (DMG) Beacon frames (see Section III) through  $S_l = \varphi_{Sradar} / \theta_{radar}$  sectors within a confined area (shown by Radar in Fig. 1), allowing the BS to obtain an estimation of the locations and velocities while providing the vehicles with

TABLE I  
PARAMETER VALUES FOR NUMERICAL EXPERIMENTS

Parameters		Value
Transmission power	$P_{tx}$	10 dBm
Path-Loss exponent	$n$	2.66
Channel attenuation	$C_{att}$	70 dB
Atmospheric attenuation	$A_{att}$	15 dB km <sup>-1</sup>
Rain attenuation	$R_{att}$	25 dB km <sup>-1</sup>
Noise Floor	$N_{floor}$	-174 dBm
Bandwidth	$B$	2.16 GHz
Carrier frequency	$f_c$	60 GHz
Wavelength	$\lambda_c$	5 mm
Noise figure	$NF$	6 dB
Max. Velocity	$v_{max}$	30 m/s
BS coverage angle	$\phi_{BS}$	120 degrees
BS-Road distance	$d$	100 m
Communications beamwidth	$\theta_{az}$	3 degrees
Outage		2 %
Initiator number of sectors (802.11ad)	$S_I$	32
Responder number of sectors (802.11ad)	$S_R$	32
Number of A-BFT slots		4

synchronization information. The duration of the radar slot is characterized in (7) and (21). At the end of the BTI and after the radar call, the BS detects each car location, and then sends a DMG beacon to each vehicle assigning them to an A-BFT slot (in order to avoid inefficient contention during legacy 802.11ad). The BS antenna is included in this message to allow the vehicles to calculate the best transmit sector. Upon BTI completion, vehicles start the Response Phase and transmit through their  $S_R$  sectors. However, they will already know BS location, therefore  $S_R = 1$ .

In summary, we perform two steps with only one transmission (radar and synchronization) during the BTI. Furthermore, we reduce the A-BFT slots by confining the BTI within the area defined by  $\varphi_{Sradar}$  and eliminate the BRP through the high localization accuracy acquired by the radar in the DTI period. The radar detects vehicles passing by a pre-defined sector and estimates their position and velocity,  $\hat{d}_i(t)$  and  $\hat{v}_i(t)$ , at a given time  $t$ . In this section, we detail (i) setting up the periodic sweep interval between consecutive sweeps, (ii) selecting sectors for the radar sweep, and (iii) allotting the time per sweep, i.e., decide the number of packets  $P$  that should be transmitted to achieve a desirable accuracy.

• **Sweep interval:** The minimum elapsed time,  $T_{radar,i}$ , between two consecutive sweeps across the same  $i$ th sector, must be set such that every vehicle which passes over that sector is detected.  $T_{radar,i}$  (17) is restricted by the sector length,  $r_i$ , and the maximum velocity expected in a vehicle,  $v_{max}$ .

$$T_{radar,i} \leq \frac{r_i}{v_{max}}. \quad (17)$$

• **Sector location:** The radar sector length,  $r_i$  (18), is defined as the road length covered by the radar, which can be expressed as a function of  $\varphi_{Sradar}$ ,  $\phi_{BS}$  and the radar sector starting angle,  $\theta_{start}$  (see Fig. 1).

$$r_i = d \left[ \tan \left( \frac{1}{2} \phi_{BS} - \theta_{start} \right) - \tan \left( \frac{1}{2} \phi_{BS} - (\theta_{start} + \varphi_{Sradar}) \right) \right]. \quad (18)$$

We simplify the analysis by restricting the number of radar sectors to one. Thus,  $\theta_{start}$  and  $\varphi_{Sradar}$  have to be determined for that single sector. Also, as vehicles must be detected as soon as

they enter the coverage area for efficient resource utilization, consider the case where the radar sector is defined by  $\theta_{start} = 0$ . Now, the system needs to impose new restrictions towards setting  $\varphi_{Sradar}$ : (i) the sector length covered by radar is not smaller than the length of the vehicle,  $w_{car}$  (19), and (ii) the distance that a vehicle may move during a radar sweep cannot be larger than a set value ( $k_2$ ) (20). The location of the  $l$ th vehicle at a given time  $t$  is denoted by  $y_l(t)$ . Two qualitative constraints defined by constants  $k_1$  and  $k_2$  are included below for flexibility in the analysis.

$$r > k_1 \cdot w_{car}, \quad (19)$$

$$[y_l(t + t_{radar}) - y_l(t)] < k_2. \quad (20)$$

Suppose the radar is configured to scan the whole area at once. To achieve a Doppler resolution of 1.5 m/s, incurring a 5% error on the velocity estimation in the worst case, the system would require around 400 ms to complete the beam alignment procedure. This is not viable, since a vehicle that was detected at the very beginning would have covered 12 m upon completion of the radar function (20). Therefore, the radar is employed only in a reduced area.

Consider a  $\varphi_{Sradar}$  of  $5^\circ$ , a  $\Delta\nu = 0.454$  m/s and a  $w_{car} \approx 5$  m. This values would correspond to  $r \approx 30$  m ( $\approx 6w_{car}$ ) and an in-radar-measure moved distance around 1.75 m ( $\approx w_{car}/3$ ). This is a numerical example of fair values for  $\varphi_{Sradar}$  and  $\Delta\nu = 0.454$  m/s according to the constraints (19)-(20).

• **Sweep time:** We define  $\rho$  as the ratio between the time taken to perform a full sweep of the chosen sector,  $t_{radar}$ , and the overall interval between sweeps  $T_{radar}$ :

$$\rho = \frac{t_{radar}}{T_{radar}}, \quad (21)$$

$$\rho(\varphi_{Sradar}, \theta_{start}) = \frac{\varphi_{Sradar} \cdot \lambda_c \cdot v_{max}}{\Delta\nu \cdot r(\varphi_{Sradar}, \theta_{start})}, \quad (22)$$

where (22) is obtained by substituting (7) and (17) into (21).

## VI. PERFORMANCE EVALUATION

Consider the scenario defined in Section V and represented in Fig. 4, where vehicles will synchronize with the BS through the procedure defined in Section V. We simulated this operation in MATLAB using the PHY parameters defined in the WLAN Systems Toolbox and Table I. We compared the overhead between the legacy 802.11ad and our modified configuration using 802.11ad-based Radar.

Fig. 6 shows  $\rho$  as a function of  $\varphi_{Sradar}$  for different fixed initial locations  $\theta_{start}$ . The configuration that provides highest radar efficiency by minimizing  $\rho$  is  $\theta_{start} = 0$ . As mentioned in Section V, this aids in the detection of cars as soon as they enter the coverage area. Therefore, placing the radar sector at the edge of the coverage area is the optimal choice.

As stated in Section V, we employ beam-overlapping to mitigate potential radar estimation errors. In Fig. 7, the impact of the Doppler resolution ( $\Delta\nu$ ) and beam-overlap on the misalignment probability is presented. Accurate velocity estimations require low  $\Delta\nu$ . However, as seen in Fig. 3, improved radar accuracy implies longer radar transmission periods. We now study the beamforming time to observe the reduction in the overhead over baseline 802.11ad. Fig. 7c

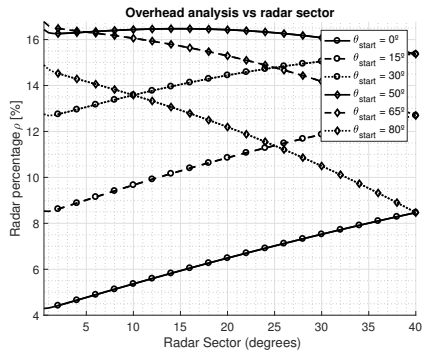


Fig. 6. Sweep time  $\rho$  as function of  $\varphi_{\text{Sradar}}$  with  $\Delta\nu = 0.456$  m/s.

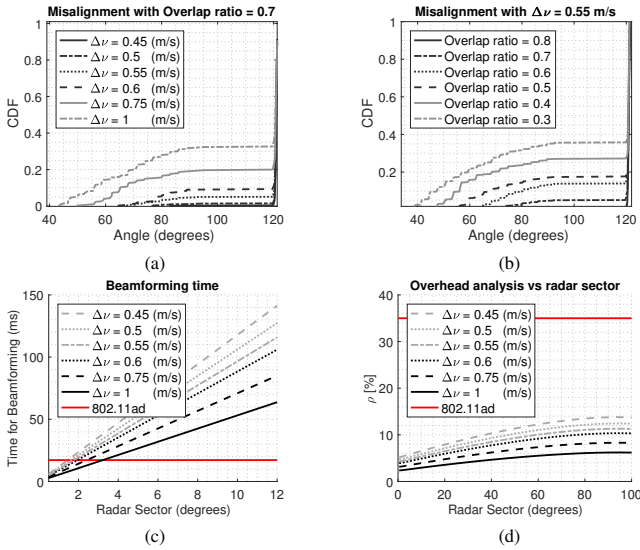


Fig. 7. Misalignment cumulative probability density function (CDF) for (a) different Doppler resolutions and (b) overlap ratios. The outage tolerance is 2%. (c) The time incurred for beamforming in one BHI worsens with radar. (d) The time spent performing beamforming is reduced because of its longer periodicity

shows the time a single beamforming procedure requires in terms of  $\varphi_{\text{Sradar}}$ . Even if the radar increases the beamforming time for a single BHI, as per (17), we only repeat this procedure every  $T_{\text{radar}}$ . In contrast, legacy 802.11ad for V2I requires such a repetition every  $\approx 30$  ms [2], which implies  $\approx 35\%$  of the overall access time. Fig. 7d shows the percentage time (22) our configuration requires of the total time.

Consider a radar design with a  $\Delta\nu$  of 0.45 m/s and a  $\varphi_{\text{Sradar}}$  of  $5^\circ$ . For a cumulative misalignment probability of less than 1% at the end of the coverage area, an overlap ratio of 0.7 is employed. This implies a beam training overhead in the BHI of 59 ms in contrast to the 10.72 ms of the 802.11ad. However, our design introduces a total overhead of 5.82% compared to the 35% from the standard. Thus, we achieve a reduction of 83% on the 802.11ad beam training overhead.

## VII. CONCLUSION

This work demonstrates the feasibility for using radar and communications jointly within a single 802.11ad transceiver

chain for high bandwidth and mobility situations. We configured the 802.11ad MAC to embed radar operations with standards-compliant packets and at the same time, improve upon the completion time and scalability of legacy beam training procedures. We have studied the ideal parameter settings for the radar operation, including the impact of varying the sweep overlap and the achievable Doppler resolution.

## ACKNOWLEDGMENTS

Kumar Vijay Mishra acknowledges partial support via Andrew and Erna Finci Viterbi Postdoctoral Fellowship and Lady Davis Postdoctoral Fellowship.

## REFERENCES

- [1] *Wireless LAN Medium Access Control (MAC) and Physical Layer (PHY) Specifications Amendment 3: Enhancements for Very High Throughput in the 60 GHz Band*, IEEE Std. 802.11ad, 2012.
- [2] I. Mavromatis, A. Tassi, R. J. Piechocki, and A. Nix, "Beam alignment for millimetre wave links with motion prediction of autonomous vehicles," in *IET Colloquium on Antennas, Propagation and RF Technology for Transport and Autonomous Platforms*, 2017, pp. 1–8.
- [3] K. V. Mishra and Y. C. Eldar, "Sub-Nyquist channel estimation over IEEE 802.11ad link," in *IEEE International Conference on Sampling Theory and Applications*, 2017, pp. 355–359.
- [4] P. Kumari, N. González-Prelcic, and R. W. Heath Jr., "Investigating the IEEE 802.11ad standard for millimeter wave automotive radar," in *IEEE Vehicular Technology Conference - Spring*, 2015, pp. 1–5.
- [5] Y. M. Tsang, A. S. Poon, and S. Addepalli, "Coding the beams: Improving beamforming training in mmWave communication system," in *IEEE Global Telecommunications Conference*, 2011, pp. 1–6.
- [6] Z. Weixia, G. Chao, D. Guanglong, W. Zhenyu, and G. Ying, "A new codebook design scheme for fast beam searching in millimeter-wave communications," *China Communications*, vol. 11, no. 6, pp. 12–22, 2014.
- [7] V. Va, T. Shimizu, G. Bansal, and R. W. Heath Jr., "Beam design for beam switching based millimeter wave vehicle-to-infrastructure communications," in *IEEE International Conference on Communications*, 2016, pp. 1–6.
- [8] N. González-Prelcic, R. Méndez-Rial, and R. W. Heath Jr., "Radar aided beam alignment in MmWave V2I communications supporting antenna diversity," in *IEEE Information Theory and Applications Workshop*, 2016.
- [9] J. George, K. V. Mishra, C. M. Nguyen, and V. Chandrasekar, "Implementation of blind zone and range-velocity ambiguity mitigation for solid-state weather radar," in *IEEE Radar Conference*, 2010, pp. 1434–1438.
- [10] K. V. Mishra, V. Chandrasekar, C. Nguyen, and M. Vega, "The signal processor system for the NASA Dual-frequency Dual-polarized Doppler Radar," in *IEEE International Geoscience and Remote Sensing Symposium*, 2012, pp. 4774–4777.
- [11] D. H. Nguyen and R. W. Heath Jr., "Delay and Doppler processing for multi-target detection with IEEE 802.11 OFDM signaling," in *IEEE International Conference on Acoustics, Speech, and Signal Processing*, 2017, pp. 3414–3418.
- [12] D. Cohen, K. V. Mishra, and Y. C. Eldar, "Spectrum sharing radar: Coexistence via Xampling," *IEEE Transactions on Aerospace and Electronic Systems*, vol. 29, pp. 1279–1296, 3 2018.
- [13] K. V. Mishra, A. Zhitnikov, and Y. C. Eldar, "Spectrum sharing solution for automotive radar," in *IEEE Vehicular Technology Conference - Spring*, 2017, pp. 1–5.
- [14] E. Grossi, M. Lops, L. Venturino, and A. Zappone, "Opportunistic automotive radar using the IEEE 802.11ad standard," in *IEEE Radar Conference*, 2017, pp. 1196–1200.
- [15] V. Va, X. Zhang, and R. W. Heath Jr., "Beam switching for millimeter wave communication to support high speed trains," in *IEEE Vehicular Technology Conference - Fall*, 2015, pp. 1–5.